Adaptive Weighted Sensing With Simultaneous Transmission for Dynamic Primary User Traffic

Min Deng, Bin-Jie Hu, *Senior Member, IEEE*, and Xiaohuan Li

***Abstract*— In practical scenarios with random arrival and departure of primary users (PUs), existing simultaneous sensing and transmission schemes allocated the same weight to each sample, and did not consider low signal-to-noise ratio (SNR) situations. This paper proposes an adaptive weighted sensing scheme with simultaneous transmission for dynamic PU traffic. It uses a power function based on the corresponding sampling sequence and could reveal the actual PU state in near real time. The power exponent is further adjusted to the sensing situations to achieve lowest false alarm probability under a certain detection probability constraint. Then, an analytical model considering all possible PU state transitions is developed to evaluate achievable interference, throughput, and energy efficiency. Furthermore, the optimal frame duration yielding both optimal false alarm probability and throughput is computed. After that, a fast search algorithm is proposed to track the optimal duration at an exponential convergence rate. Simulation results are provided to validate the analytical model and demonstrate the improvement in low SNR. The results indicate that the proposed scheme can achieve lower false alarm probability and higher energy efficiency over a wide SNR range than that of the existing weighting schemes, which are based on probability, geometric sequence, and equal weighting.**

***Index Terms*— Cognitive radio, spectrum sensing, weight, full duplex, optimization.**

I. Introduction

COGNITIVE radio (CR) is a promising technique to ameliorate the spectrum utilization efficiency by intelligently exploiting the spectrum holes (idle bands) without causing intolerable interference to primary users (PUs) [1]–[3]. Spectrum sensing plays a crucial role in periodically detecting the presence or absence of PU signals and deciding whether the secondary user (SU) can access the given spectrum or not [4], since spectrum holes are dynamically scattered and may not remain available for a long time in the dynamic PU traffic environment.

Most spectrum sensing works are based on conventional frame structure defined in the IEEE 802.22 proposal. According to it, a short quiet period is arranged at the beginning of each frame for sensing the state of the band [5]. On one hand, SU must balance between PU protection and SU throughput [6]. In fact, the sensing duration should be short to leave more time for transmission, but long enough to ensure the sensing accuracy. On the other hand, the insertion of quiet periods causes additional burden on synchronization between PU and SU.

In view of above problems, some research works have been conducted on simultaneous sensing and transmission. Active sensing was proposed as an alternative to remove intra-frame quiet periods and synchronization, where sensing is performed by some inactive SUs with eigenvalue detection [7], [8], cyclostationary feature detection [9] or energy detection [10]. However, inactive SUs are forced to consume extra power and spectrum resources in sensing and sending information to active ones. Besides, the results may not be accurate due to different locations between the sensing and active SUs. Hence, it's more beneficial to perform sensing and transmitting concurrently on the same CR device through in-band full-duplex (FD) operation [11]. Recently, significant progress in antenna isolation and self-interference suppression (SIS) has presented great promise for realizing FD communications [12], [13]. Spectral-energy efficiency tradeoff in a FD two-way relay network was studied by considering the residual SI at the relay in [14]. Energy detection with both two-antenna and single-antenna FD transceivers in the presence of residual self-interference was concerned in [15]. The authors in [16]–[19] proposed a novel frame and receiver structure to conduct sensing and transmitting at the same time. Since the whole frame duration is used both for sensing and transmitting, detection performance and throughput can be improved simultaneously. Furthermore, interweave spectrum sharing systems were presented in [20]–[22]. It used power control to further improve throughput.

However, all the above mentioned researches allocate equal weights to each sample. In practical scenario, channel state may change during the sensing period. Moreover, the received energy at SU may change suddenly between consecutive observations. That's because the arrival and departure of PU signals is random. Thus heavier weights should be assigned to the latest samples, which represent the more actual PU's state.

There are two main weighted sensing schemes that can reflect temporal difference between samples. One is based on the probability of the presence/absence of PU at the corresponding sample. Quiet sensing based on this scheme was performed in [23] without considering the probability of the leaving of PU. While the authors in [24] gave

Manuscript received February 17, 2016; revised July 30, 2016 and November 15, 2016; accepted January 6, 2017. Date of publication January 16, 2017; date of current version March 15, 2017. This work was supported by the IOT Key Project of the Ministry of Industry and Information Technology ([2014]351), Guangzhou key science and technology project of Industry-Academia-Research collaborative innovation (2014Y2-00218), University-Industry Key Project of Department of Education of Guangdong Province (CGZHZD1102). The associate editor coordinating the review of this paper and approving it for publication was H. Li. *(Corresponding author: Bin-Jie Hu.)*

The authors are with the School of Electronic and Information Engineering, South China University of Technology, Guangzhou 510640, China (e-mail: d.min03@mail.scut.edu.cn; eebjiehu@scut.edu.cn; xhuanlee@126.com).

Color versions of one or more of the figures in this paper are available online at http://ieeexplore.ieee.org.

Digital Object Identifier 10.1109/TCOMM.2017.2652460

further analysis based on PU's access/leave probability model. However, the unnormalized weights lead to large threshold scope and become unsuitable for low signal-to-noise ratio (SNR) conditions. The other weighted sensing scheme is based on geometric sequence. Sensing performance with different common ratios was given to show the eclectic one in [25] in FD scenario with SIS. Similar normalized weighting schemes with conventional frame structure were proposed in [26] and [27]. They adopted a nature exponential common ratio and a dynamic ratio adapted to PU transition activity, respectively. All these methods performed well with a small number of samples in high SNR (above 0 dB) conditions. However, they did not consider low SNR conditions. In generally, the low SNR of PU signals is unavoidable. The reason is that multipath fading and shadowing phenomena result in power fluctuations of received PU signals. Furthermore, in low SNR scenarios, the required number of samples has to be large enough to achieve a satisfactory performance. It is likely to exceed computing limit since their common ratios are relatively big.

To improve the performance over a wide range of SNR levels, we design a power function based weighting scheme for energy detection in the dynamic PU traffic environment. It puts heavier weights to the newer samples, making the test statistic reflect the actual PU state better. The power exponent is further adjusted to the sensing situations to achieve lowest false alarm probability under a certain detection probability constraint. Considering all possible PU state transitions, we analyze the performance of sensing accuracy, interference, throughput and energy efficiency. Interweave spectrum sharing and a frame structure of simultaneous sensing and transmission are adopted to achieve higher throughput by making full advantage of FD radios. Although the frame structure can overcome the sensing-throughput tradeoff [17], we find that a longer frame duration does not yield a better performance. It motives us to study the design of optimal frame duration.

The main contributions of this paper are as follows.

- A novel adaptive weighted spectrum sensing scheme based on a power function in the dynamic PU traffic environment is proposed to improve the sensing performance in low SNR conditions.
- All possible PU states are considered in the system model to evaluate the sensing performance.
- We prove the existence of an optimal frame duration with the adopted frame structure.
- A heuristic search algorithm is proposed to find the optimum frame duration at an exponential convergence rate.
- Simulation results verify the feasibility of proposed algorithm and show the improvements in sensing accuracy, throughput and energy efficiency in low SNR conditions compared with the state of arts without increasing the order of the computational complexity.

The remainder of this paper is organized as follows: Section II presents a system model for spectrum sensing. Then, the proposed weighted sensing scheme and the corresponding weight optimization formulation are presented in Section III. In Section IV we study the spectrum sensing performance considering the PU state switch and solve the frame duration optimization problem. Numerical results are shown in Section V to validate the observations and evaluate the performance. Finally Section VI concludes this paper.

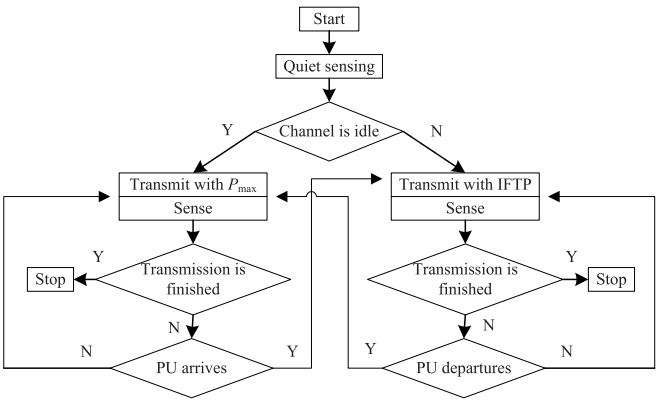

Fig. 1. Spectrum sensing and transmitting framework with FD/SIS.

II. System Model

In this paper, we consider the scenario of a single SU attempting to sense and access the PU channel in interweave sharing pattern. SU is equipped with FD radios with SIS ability [19]. The spectrum sensing framework is depicted in Fig. 1.

When SU needs to transmit, it performs quiet sensing with conventional wireless half-duplex based frame structure at first. If the decision shows the absence of PU signal at present, SU begins to transmit with the maximum power. Otherwise, an interference-free transmitting power (IFTP) is adopted [28]. During transmission, sensing is conducted simultaneously based on the frame structure of simultaneous sensing and transmission in case of PU state changes. Thus the whole frame duration T can be utilized for both sensing and transmitting. The SU cancels the signal sent by SU's transmitter by SIS from the received signal, and uses the remainder to perform sensing. Sensing decision is made circularly at the end of every frame, and SU adjusts the transmit power accordingly. If the decision indicates the presence of PU signal, SU adopts an IFTP estimated by spatial spectrum sensing. In this way, the continuity of SU's data transmission can be facilitated. This process repeats until SU finishes its data transmission.

Here we consider a more practical scenario where the PU traffic is dynamic, and the PU and SU are asynchronous. Therefore, the energy values received currently are more likely to reveal actual PU state than the earlier ones. In order to detect the PU state change sensitively, T should be limited. In this case, we presume that the PU state changes at most once during T.

We adopt the popular energy detection technique [29] in CR network, owing to its efficiency and low implementation complexity. More importantly, it requires no prior information of received PU signal, which typically may not be known to SUs. Under the wireless-FD mode, the received signal from the band of interest at time t, denoted by $y(t)$, can be expressed as

$$y(t) = \sqrt{k}s(t) + n(t). \tag{1}$$

where $s(t)$ is the PU signal, which is an independent and identically distributed (i.i.d.) random circularly symmetric complex Gaussian (CSCG) signal, and $n(t)$ represents the i.i.d. CSCG noise with zero mean and variance of σ_n^2. Without loss of generality, we assume that PU signal is independent of the noise signal. We use the coefficient k ($k \in [0, 1]$) to quantify the impact of SIS on the FD communication. Specifically, if $k = 1$, SU can totally suppress self-interference signal (i.e., perfect SIS). Otherwise, only a fraction of the self-interference can be suppressed (i.e., imperfect SIS). In our system, we consider the latter regime to make it more practical.

Then, since PU may arrive and departure randomly, the received energy value by equal weighting in a frame period can be expressed as

$$Y(y) = \begin{cases} \frac{1}{N}\left(\sum_{i=1}^{g} |\sqrt{k}s(i) + n(i)|^2 + \sum_{i=g+1}^{N} |n(i)|^2\right), & H_{10} \\ \frac{1}{N}\left(\sum_{i=1}^{r} |n(i)|^2 + \sum_{i=r+1}^{N} |\sqrt{k}s(i) + n(i)|^2\right), & H_{01} \end{cases} \tag{2}$$

where $N = Tf_s$ implies the number of samples for the entire sensing duration with the sampling frequency f_s; H_{10} represents that PU is active for previous g ($1 \le g \le N-1$) samples and then becomes inactive afterwards; H_{01} represents that PU is inactive for r ($1 \le r \le N-1$) samples at first but becomes active later. When $g = 0$ ($r = 0$), it means PU signal keeps absent (present) during the entire sensing period, which can be represented as the static PU traffic situation H_{00} (H_{11}). Sensing decision can be made by comparing the test statistics with a decision threshold. Since PU state may change over the sensing period, we need to consider the state of PU at the last moment. Detection probability (p_d) should be redefined as the probability that sensing decision declares the channel as busy under situations of both H_{01} and H_{11}, for PU signal is still present at the end of the sensing period. Similarly, false alarm probability (p_f) should be defined as the probability that sensing decision indicates the channel to be busy under situations of both H_{10} and H_{00}, for PU signal is absent at the end of the sensing period.

III. Proposed Weighted Spectrum Sensing Schemes

For static PU activity, the optimal weight scheme is equal weighting [26] by using standard Lagrange multiplier. However, in dynamic PU activity environment, samples received earlier can be counterproductive. Therefore a more efficient way is to assign heavier weights to newer samples. In this section, we design a novel weighting scheme by using power function, making the newer samples contribute more to the decision statistics. Furthermore, the power exponent is adjusted to get lowest false alarm probability under a certain detection probability constraint.

A. Power Function-Based Weighting Scheme

When PU signal appears randomly, it's no longer realistic to assume PU state keeps constant over the sensing period. The samples at the end of the period are more likely to reveal actual PU state while samples at the beginning may not. Therefore a natural thinking is to assign bigger weight to the newer samples. Some researchers have noticed the principle recently. Weights are set as the geometric sequence in [25], [26]. They work excellently with small N when SNR is above 0 dB. However, it's computational demanding especially when acquired N is large in low SNR condition. Thus it's very likely to exceed computing limit with a relatively large common ratio. Besides, the unnormalized weights result in large threshold scope, making it less feasible.

Inspired by that, we consider a less complex weighting scheme in a form of power function as shown in (3). The weight w_{fi} is applied to the corresponding sample with time index i:

$$w_{fi} = \frac{i^f}{\sum_{i=1}^{N} i^f}, \quad i = 1, 2, \cdots, N. \tag{3}$$

The power exponent f ($f \ge 0$) can be chosen properly. When $f = 0$, it reduces to equal weighting. The sum of the weights equals 1, which facilitates the threshold searching. Since w_{fi} increases with i, the weights allocated for newer samples are heavier than those for earlier ones. In this way, if PU state changes in the sensing period, the samples received after the change can make more contributions to the decision. Thus the sensing accuracy can be improved. It's easy to see that the acquired number of multiplications is less than that of the geometric sequence based weights. What's more, even if N is large in low SNR conditions, it is hard to exceed the computing limit. Thus the weighting scheme is robust and feasible. We can obtain the decision statistics in a frame period under H_{10} and H_{01} easily by substituting w_{fi} for $1/N$ in (2).

When N is relatively large, using the central limit theorem, the probability density function of $Y(y)$ can be approximated by a Gaussian distribution [29]. Note that a weighted sum of Gaussian random variables is also a Gaussian random variable. Let η and γ_p be the energy detection threshold and received SNR of PU respectively, we can express the probabilities of detection and false alarm as in (4) with weighted mean and variance [6], [19]:

$$\begin{cases} P_{fH_{10}}(g) = Q\left(\dfrac{\frac{\eta}{\sigma_n^2} - \sum_{i=1}^{g} w_{fi}(k\gamma_p + 1) - \sum_{i=g+1}^{N} w_{fi}}{\sqrt{\sum_{i=1}^{g} w_{fi}^2(k\gamma_p + 1)^2 + \sum_{i=g+1}^{N} w_{fi}^2}}\right), \\ P_{dH_{01}}(r) = Q\left(\dfrac{\frac{\eta}{\sigma_n^2} - \sum_{i=1}^{r} w_{fi} - \sum_{i=r+1}^{N} w_{fi}(k\gamma_p + 1)}{\sqrt{\sum_{i=1}^{r} w_{fi}^2 + \sum_{i=r+1}^{N} w_{fi}^2(k\gamma_p + 1)^2}}\right), \end{cases} \tag{4}$$

where $Q(\cdot)$ is the complementary distribution function of the standard Gaussian.

From SU's perspective, lower p_f means more chances to reuse the spectrum holes. However, in order to provide sufficient protection of PUs, constraining p_d can be more appropriate than fixing p_f. This approach is referred as

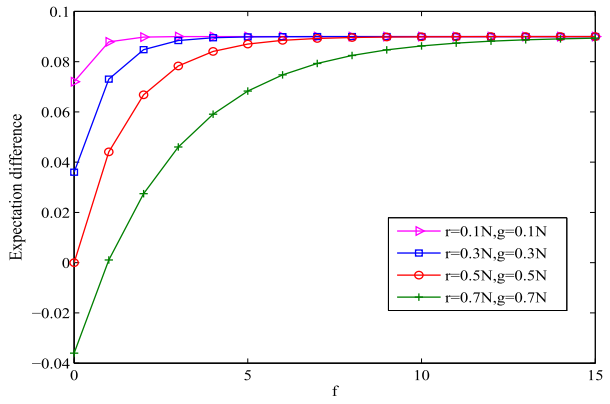

(a) Expectation difference

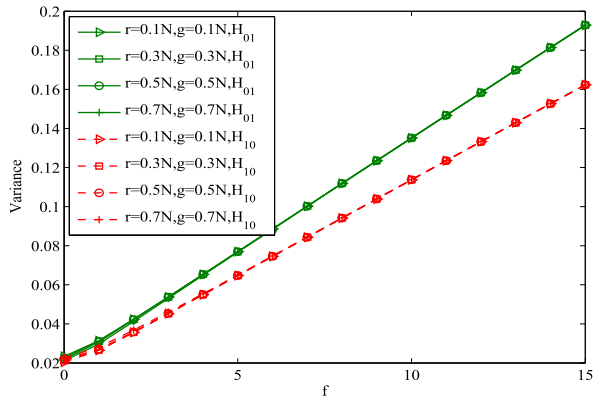

(b) Variances

Fig. 2. The expectation difference and variances under H_{01} and H_{10}. $k = 0.9$, $\gamma_p = -10$ dB, $N = 1000$.

constant detection rate (CDR) design strategy [30], where the threshold must guarantee that p_d is higher than a given target detection probability p_{d_con}. Since $Q(\cdot)$ is a monotonically decreasing function, lowest p_f can be achieved with a largest threshold, which corresponds to the situation when the equality constraint $p_d = p_{d\_con}$ is satisfied.

Apparently, the moments r and g that PU state changes during a sensing period can significantly affect the sensing performance. If r or g is small, PU changes its state early, leaving more samples that can reflect the real-time PU state in the end. While r or g grows larger, more samples become outdated and counterproductive, degrading the sensing accuracy.

Furthermore, the value of f makes great influence on the sensing performance. According to the probability density function of the weighted energy values [6], [19], it's easy to see that the variances of the test statistics increase with f (see Fig. 2). For convenience, let the variance of noise $\sigma_n^2 = 1$. Let α be the difference between the expectations of the distributions H_{01} and H_{10}, which can be derived as

$$\alpha = k\gamma_p \left(\sum_{i=r+1}^{N} i^f - \sum_{i=1}^{g} i^f \right) / \sum_{i=1}^{N} i^f \tag{5}$$

It is easy to obtain the first derivation of α with respect to f, which is larger than or equal to 0. Thus α increases

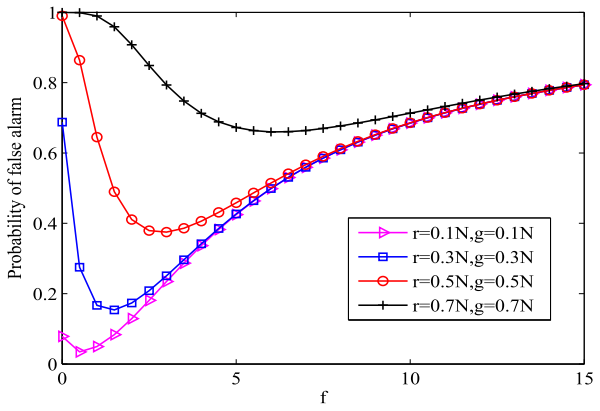

Fig. 3. False alarm probability under H_{01} and H_{10}. $k = 0.9$, $\gamma_p = -10$ dB, $N = 3000$.

with f and finally saturates (see Fig. 2). Obviously, the smaller the overlapped area of the distributionsH_{01} and H_{10} is, the better the detection accuracy can achieve [27]. The size of the overlapped area decreases when the expectation difference α increases and the corresponding variances decrease. Thus, detection accuracy improves with α, but degrades with the variances of the statistics. Considering the influence of f, we can see that with the increase of f, the increasing α makes the detection accuracy improve at first, for the variances haven't increased too much. Then, the increase of α becomes less and less. While the variances increase rapidly. Actually, assigning heavier weights (by using larger f) to samples at the end affects the statistical stability [26]. When the gain achieved from larger α can't counteract the degradation caused by the statistical unstability (larger variances), the performance could get degraded. Thus there exists a tradeoff between the gain from larger expectation difference and degradation from larger variance of test statistics when f increases. An optimum f can make the test statistics achieve large expectation difference and small variances, leading to a minimum false alarm probability. Besides, the optimum f differs as the PU's state varies. This can be verified by Fig. 3.The false alarm probability and the optimization of f are discussed from a mathematical point-of-view in the following subsection.

B. Adaptive Weighted Spectrum Sensing

Mathematically, in order to find the optimal power exponent yielding the lowest p_f intelligently in case of the sensing scenario changes, we formulate the following optimization problem

$$\min_{f} \; P_{fH_{10}} \quad \text{s.t.} \begin{cases} P_{dH_{01}} \geq P_{d\_con}, \\ 0 \leq f \leq f_{max}. \end{cases} \tag{6}$$

Here we restrict the upper boundary of power exponent f_{max} to avoid exceeding calculating limit when the number of samples gets too large. In fact, f_{max} can be adjusted according to related sensing scenario to narrow down the search range and speed up the searching. Since the lowest false alarm probability can be achieved when the equality

constraint of detection probability is satisfied, we can obtain the corresponding expression of optimum threshold. With the obtained threshold, the objective function can be expressed by (7) after simple mathematical manipulations, where $\Delta = \sum_{i=1}^{r} i^{2f} + \sum_{i=r+1}^{N} i^{2f}(k\gamma_p+1)^2$, $\theta = Q^{-1}(P_{d\_con})$

$$P_{fH_{10}} = Q\left(\frac{\theta\sqrt{\Delta} + k\gamma_p\left(\sum_{i=r+1}^{N} i^f - \sum_{i=1}^{g} i^f\right)}{\sqrt{\sum_{i=1}^{g} i^{2f}(k\gamma_p+1)^2 + \sum_{i=g+1}^{N} i^{2f}}}\right). \quad (7)$$

According to the IEEE 802.22 standard, the target detection probability P_{d_con} should be higher than 0.9 to protect PUs sufficiently. Considering the decreasing property of $Q(\cdot)$, θ should be smaller than -1.28. While for low SNR and imperfect SIS regime, both γ_p and k should be smaller than 1. Thus it's easy to see that $P_{fH_{10}}$ is convex in the range of f, which can be confirmed by Fig. 3. Let S denote the term inside the parentheses of $Q(\cdot)$, and $\nu = \sum_{i=1}^{g} i^{2f}(k\gamma_p+1)^2 + \sum_{i=g+1}^{N} i^{2f}$. Then the first derivative of $P_{fH_{10}}$ with respect to f can be derived as

$$P'_{fH_{10}f} = \frac{-\exp(S^2/2)}{\sqrt{2\pi}} S'_f, \quad (8)$$

where

$$\begin{aligned} S'_f = {} & \frac{\theta(\sum_{i=1}^{r} i^{2f}\ln(i) + \sum_{i=r+1}^{N} i^{2f}\ln(i)(k\gamma_p+1)^2)}{\sqrt{\Delta}\sqrt{\nu}} \\ & + \frac{k\gamma_p(\sum_{i=r+1}^{N} i^f \ln(i) - \sum_{i=1}^{g} i^f \ln(i))}{\sqrt{\nu}} \\ & + \frac{\theta\sqrt{\Delta} + k\gamma_p(\sum_{i=r+1}^{N} i^f - \sum_{i=1}^{g} i^f)}{\nu^{3/2}} \\ & \times (\sum_{i=1}^{g} i^{2f}\ln(i)(k\gamma_p+1)^2 + \sum_{i=g+1}^{N} i^{2f}\ln(i)) \end{aligned} \quad (9)$$

is the first derivative of S with respect to f. Thus the optimal f can be obtained as the solution to $P'_{fH_{10}f} = 0$. However, it's too complicated to obtain the explicit closed-form solution f. Therefore we adopt the numerical search method by combining the golden section search technique and Lagrange quadratic interpolation to solve the optimization problem in a finite number of iterations. The implementation details are specified in Section V. In this way, the optimal f can be found efficiently as long as any parameter in the sensing scenario changes.

IV. Optimized Weighted Spectrum Sensing Considering PU State Switch

In the previous section, we have explored the conditional sensing performance of the proposed weighting scheme in arbitrary PU state change situation without considering the state transition probabilities. Here we take all the possible instants of PU state change into consideration, and obtain the optimal frame duration.

A. Sensing Model

The PU traffic activity is modeled as a two-state random process when the PU alternates between ON (1) and OFF (0) states representing busy and idle channel respectively. PU's arrival is independent, and follows the Poisson arrival process. Thus, the duration of ON (OFF) periods can be assumed to be exponentially distributed with mean of $1/\lambda$ $(1/\mu)$ [31]. Then, at any time instant, a channel is busy with probability $P_{on} = \mu/(\lambda+\mu)$, and idle with probability $P_{off} = \lambda/(\lambda+\mu)$. The state transition matrix is formulated as

$$\Phi = \begin{pmatrix} P_{00}(\tau) & P_{01}(\tau) \\ P_{10}(\tau) & P_{11}(\tau) \end{pmatrix}, \quad (10)$$

where τ denotes the sample interval. $P_{01}(\tau)$ denotes the transition probability that a channel changes its state from 0 to 1 after τ seconds, which can be expressed as

$$P_{01}(\tau) = \mu/(\lambda+\mu) - \mu/(\lambda+\mu)\exp(-(\lambda+\mu)\tau). \quad (11)$$

Similarly, other transition probabilities of channel states can be expressed as

$$P_{10}(\tau) = \lambda/(\lambda+\mu) - \lambda/(\lambda+\mu)\exp(-(\lambda+\mu)\tau), \quad (12)$$

$$P_{00}(\tau) = 1 - P_{01}(\tau), \quad P_{11}(\tau) = 1 - P_{10}(\tau). \quad (13)$$

In dynamic PU traffic environment, PU detection problem is now a quaternary hypothesis testing problem. We can express the received energy as

$$Y = \begin{cases} \sum_{i=1}^{N} w_i|n(i)|^2, & H_{00} \\ \sum_{i=1}^{g} w_i|\sqrt{k}s(i)+n(i)|^2 + \sum_{i=g+1}^{N} w_i|n(i)|^2, & H_{10} \\ \sum_{i=1}^{N} w_i|\sqrt{k}s(i)+n(i)|^2, & H_{11} \\ \sum_{i=1}^{r} w_i|n(i)|^2 + \sum_{i=r+1}^{N} w_i|\sqrt{k}s(i)+n(i)|^2, & H_{01} \end{cases} \quad (14)$$

where w_i represents the weight of the ith sample; hypothesis H_{00} and H_{11} correspond to the absence and presence of PU during the entire sensing period respectively. The conditional probabilities of detection and false alarm of hypothesis H_{01} and H_{10} can be obtained by (4). While under hypothesis H_{00} and H_{11}, they can be expressed as (15), which correspond to the weighted energy detection in static PU traffic scenario:

$$\begin{cases} P_{fH_{00}} = Q\left(\dfrac{\frac{\eta}{\sigma_n^2} - \sum_{i=1}^{N} w_i}{\sqrt{\sum_{i=1}^{N} w_i^2}}\right), \\ P_{dH_{11}} = Q\left(\dfrac{\frac{\eta}{\sigma_n^2} - \sum_{i=1}^{N} w_i(k\gamma_p+1)}{\sqrt{\sum_{i=1}^{N} w_i^2(k\gamma_p+1)^2}}\right). \end{cases} \quad (15)$$

We assume that T is quite short compared with the duration of PU state, and PU only changes its state once in one frame.

Then, the probability of each hypothesis can be written as

$$P_{H_{00}} = P_{off} P_{00}^{N}(\tau), \quad P_{H_{11}} = P_{on} P_{11}^{N}(\tau),$$
$$P_{H_{10}} = \sum_{g=1}^{N-1} P_{on} P_{11}^{g}(\tau) P_{10}(\tau) P_{00}^{N-g-1}(\tau),$$
$$P_{H_{01}} = \sum_{r=1}^{N-1} P_{off} P_{00}^{r}(\tau) P_{01}(\tau) P_{11}^{N-r-1}(\tau). \quad (16)$$

Equation (14) indicates that false alarm occurs possibly during H_{00} and H_{10}, as only noise is present at the end of the sensing frame. While there is a possible missed detection of PU signal during H_{11} and H_{01}. Considering all cases of the PU state switch, the average probability of false alarm can be obtained by averaging the conditional probabilities of false alarm in (4) and (15) over the probabilities of occurring H_{00} and H_{10} in (16) as [32]

$$P_f = \frac{P_{H_{00}} P_{fH_{00}}}{P_{H_{00}} + P_{H_{10}}} + \frac{\sum_{g=1}^{N-1} P_{on} P_{11}^{g}(\tau) P_{10}(\tau) P_{00}^{N-g-1}(\tau) P_{fH_{10}}(g)}{P_{H_{00}} + P_{H_{10}}}. \quad (17)$$

where $\frac{P_{H_{00}}}{P_{H_{00}}+P_{H_{10}}}$ can be taken as a weighting factor that considers the case when H_{00} occurs, $\frac{P_{H_{10}}}{P_{H_{00}}+P_{H_{10}}}$ can be seen as a weighting factor when H_{10} occurs. But since the conditional false alarm probability $P_{fH_{10}}$ depends on g, the summation notation of $P_{H_{10}}$ is moved to the outside.

Similarly, the average probability of detection can be obtained by averaging the conditional probabilities of detection in (4) and (15) over the probabilities of hypotheses H_{11} and H_{01} in (16) as [32]

$$P_d = \frac{P_{H_{11}} P_{dH_{11}}}{P_{H_{11}} + P_{H_{01}}} + \frac{\sum_{r=1}^{N-1} P_{off} P_{00}^{r}(\tau) P_{01}(\tau) P_{11}^{N-r-1}(\tau) P_{dH_{01}}(r)}{P_{H_{11}} + P_{H_{01}}}. \quad (18)$$

Again, we can use the threshold that satisfies the constraint $P_d = P_{d\_con}$ to obtain lowest P_f.

B. Analysis of Interference and Outage

It's important to make sure that the interference and outage is tolerable for PU [22], [33]. Our analysis conservatively considers any time overlap between PU and SU transmissions as outage, unless an IFTP is adopted for SU [28]. In dynamic PU traffic environment, the interference and outage can possibly occur in the following cases:

Case I: when PU is present initially, but SU falsely decides that PU is absent, collision will occur, for maximum power will be used. In this case, collision has two patterns according to the activity of PU, as shown in Fig. 4(a), where the shadow area indicates the presence of PU. The left figure depicts the collision over the entire period. The right figure describes the collision before PU departures. Obviously, the overlapping time depends on the moment of PU's departure.

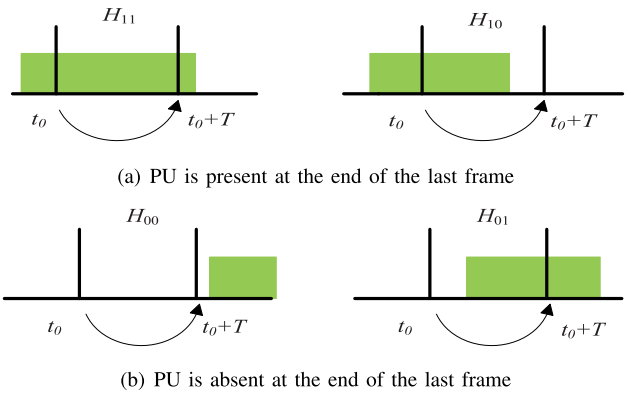

(a) PU is present at the end of the last frame

(b) PU is absent at the end of the last frame

Fig. 4. Interference model in dynamic PU traffic environment.

Considering different PU states, we can express the interference due to missed detection as

$$P_{I\_m} = P_{on}(1 - P_d) \times \left(P_{11}^{N}(\tau) + \sum_{g=1}^{N-1} P_{11}^{g}(\tau) P_{10}(\tau) P_{00}^{N-g-1}(\tau) \right) = (1 - P_d)(P_{H_{11}} + P_{H_{10}}). \quad (19)$$

Thus the expected overlap duration of PU and SU due to missed detection can be obtained as

$$E[T_{O\_m}] = P_{on}(1 - P_d) \times \left(P_{11}^{N}(\tau) T + \sum_{g=1}^{N-1} P_{11}^{g}(\tau) P_{10}(\tau) P_{00}^{N-g-1}(\tau) \frac{gT}{N} \right). \quad (20)$$

Case II: as shown in Fig. 4(b), PU is absent at the beginning. On one hand, if false alarm occurs, PU is deemed to be present. Then SU ceases its transmission in current channel, or continues with an IFTP in the following frame. Thus, it won't cause interference whether PU keeps absent or appears halfway. On the other hand, if SU detects the spectrum hole successfully, maximum power is adopted. Then, if PU reclaims the band at some point as shown in the right figure, collision occurs. Then the interference due to the re-occurrence of PU can be given by

$$P_{I\_r} = P_{off}(1 - P_f) \sum_{r=1}^{N-1} P_{00}^{r}(\tau) P_{01}(\tau) P_{11}^{N-r-1}(\tau) = (1 - P_f) P_{H_{01}}. \quad (21)$$

Since the outage time depends on the moment of PU's arrival, the expected overlap duration of PU and SU in this case can be represented as

$$E[T_{O\_r}] = P_{off}(1 - P_f) \times \sum_{r=1}^{N-1} \left(P_{00}^{r}(\tau) P_{01}(\tau) P_{11}^{N-r-1}(\tau) \frac{(N - r)T}{N} \right). \quad (22)$$

Thus the interference probability can be given as

$$P_{int} = P_{I\_m} + P_{I\_r}, \quad (23)$$

which is influenced by both the PU activity and the sensing performance. Because our system adopts CDR strategy, the interference induced by missed detection is negligible. Then conflicts mainly occur during SU's transmission on the temporary spectrum hole, which mainly depends on P_f, for the probability of detecting spectrum hole is $1-P_f$. Lower false alarm probability means more chances to utilize the available spectrum holes, thus more conflicts when PU reoccurs.

It's easy to know that the mean duration of PU's ON period during a frame is $T \cdot P_{on}$. By exploiting the analysis in [22], [33], the outage probability can be obtained as the ratio of the overlap duration to the total PU ON period, which can be expressed as

$$P_{out} = \Big(E[T_{O\_m}] + E[T_{O\_r}]\Big)/(T \cdot P_{on}). \tag{24}$$

Similarly, it is determined by the instant when the PU switches its state during period T (if any) and the SU's sensing outcomes.

C. Analysis of Throughput

With FD communication, we can adopt interweave spectrum sharing to achieve higher throughput. If the sensing decision indicates the return of PU, SU continues its transmission with an IFTP. Otherwise, maximum power is used to fully exploit the recognized spectrum hole. Consequently the throughput of SU can be influenced by both the sensing decision at the end of last frame and the PU activity in current frame.

On one hand, when PU is absent at the end of last frame, if SU detects the spectrum hole correctly, it transmits with maximum power. Or else, it deems the presence of PU as a false alarm, and therefore IFTP is used. There are two possible hypotheses during the current frame:

Under hypothesis H_{00}, PU keeps absent. Therefore, only the system noise presents. Let γ_s and γ_{sp} be the SNRs of the SU's transmission when maximum power and IFTP are used, respectively. Since the whole frame duration can be used for transmission, the conditional channel capacity is $C_1 = \log_2(1+\gamma_s)$ or $C_2 = \log_2(1+\gamma_{sp})$ if spectrum hole is detected or not, respectively.

Under hypothesis H_{01}, PU arrives on the channel after r samples. Therefore PU signal acts as noise during SU's transmission in the latter $(N-r)$ samples, which takes up a proportion of $(N-r)/N$ in one frame. Similarly, if the decision indicates the existence of spectrum hole, the conditional channel capacity is $C_3(r) = \log_2(1+\gamma_s/(1+(N-r)/N\gamma_p))$. Else, false alarm occurs. Thus, the conditional channel capacity is $C_4(r) = \log_2(1+\gamma_{sp}/(1+(N-r)/N\gamma_p))$.

On the other hand, when PU is present at the end of last frame, IFTP or maximum power is adopted if PU signal is correctly detected or not. There are also two possible hypotheses during current frame:

Under hypothesis H_{11}, PU is present all the time. Thus PU signal is considered as noise in the entire frame duration. Then the corresponding conditional channel capacity is $C_5 = \log_2(1+\gamma_s/(1+\gamma_p))$ or $C_6 = \log_2(1+\gamma_{sp}/(1+\gamma_p))$ if missed detection occurs or not.

Under hypothesis H_{10}, PU departures after g samples. Thus PU signal constitutes part of noise for a fraction of g/N. Analogously, the conditional channel capacity is $C_7(g) = \log_2(1+\gamma_s/(1+g/N\gamma_p))$ or $C_8(g) = \log_2(1+\gamma_{sp}/(1+g/N\gamma_p))$ if missed detection occurs or not.

Finally, we can obtain the average throughput of SU by averaging the conditional channel capacities over their respective probabilities of occurrence, and is given as

$$R = R_{H_{00}} + R_{H_{01}} + R_{H_{10}} + R_{H_{11}}, \tag{25}$$

where

$$\begin{aligned}
R_{H_{00}} &= (1-P_f)P_{H_{00}}C_1 + P_f P_{H_{00}}C_2,\\
R_{H_{01}} &= (1-P_f)\sum_{r=1}^{N-1} P_{off}P_{00}^{r}(\tau)P_{01}(\tau)P_{11}^{N-r-1}(\tau)C_3(r)\\
&\quad + P_f\sum_{r=1}^{N-1} P_{off}P_{00}^{r}(\tau)P_{01}(\tau)P_{11}^{N-r-1}(\tau)C_4(r),\\
R_{H_{11}} &= (1-P_d)P_{H_{11}}C_5 + P_d P_{H_{11}}C_6,\\
R_{H_{10}} &= (1-P_d)\sum_{g=1}^{N-1} P_{on}P_{11}^{g}(\tau)P_{10}(\tau)P_{00}^{N-g-1}(\tau)C_7(g)\\
&\quad + P_d\sum_{g=1}^{N-1} P_{on}P_{11}^{g}(\tau)P_{10}(\tau)P_{00}^{N-g-1}(\tau)C_8(g).
\end{aligned} \tag{26}$$

D. Analysis of Energy Efficiency

In interweave spectrum sharing, the total power consumption consists of three parts: circuit consumption (ϕ_c), spectrum sensing consumption (ϕ_{se}), and data transmission (ϕ_{tr}). Circuit consumption is usually approximated as a constant, representing the average power consumed by electronic devices (excluding power amplifier) such as mixers and filters. Since the time consumed by spectrum sensing is the same as the frame duration T, the sensing consumptions under four hypotheses are the same. With regard to ϕ_{tr}, it varies with the transmitting power related to the spectrum sensing decision. Let ϕ_{trs} and ϕ_{trsp} denote the transmission consumptions when the maximum power and IFTP are adopted, respectively. Considering four hypotheses, we can express the average data transmission power consumption as

$$\begin{aligned}
\phi_{tr} &= \Big((P_{H_{00}}+P_{H_{10}})(1-P_f) + (P_{H_{11}}+P_{H_{01}})(1-P_d)\Big)\phi_{trs}\\
&\quad + \Big((P_{H_{00}}+P_{H_{10}})P_f + (P_{H_{11}}+P_{H_{01}})P_d\Big)\phi_{trsp}.
\end{aligned} \tag{27}$$

Then the total energy consumption within a frame can be given as

$$E = (\phi_c + \phi_{se} + \phi_{tr})T. \tag{28}$$

Using the definition in [34], the energy efficiency can be obtained as the ratio of average throughput and energy consumption, which is given as

$$\zeta = RT/E = R/(\phi_c + \phi_{se} + \phi_{tr}). \tag{29}$$

Although the throughput can get improved compared with overlay sharing regime, the energy consumption is also increased for it has to transmit when PU is declared present.

E. Frame Duration Optimization

Although the adopted frame structure overcomes the sensing-throughput tradeoff [17], [19] without the need of an appropriate ratio between sensing and transmitting duration, we take a further step to investigate the influence of frame duration on the throughput of CR system.

With CDR sensing, the missed detection probability is negligibly small because p_{d_con} is set close to 1 to protect PU sufficiently. Besides, when the sensing decision declares the presence of PU, adopted IFTP is much lower than the maximum power. Thus the throughput is mainly dominated by the probability of detecting spectrum holes $(1-p_f)$. Lower p_f can lead to higher throughput. The lowest p_f can be achieved when the constraint of $p_d = p_{d\_con}$ is satisfied. Specifically, we analyze the influence of frame duration on p_f with equal weighting for a general PU activity model. Then the expression of p_f as a function of N can be obtained by setting f in (6) as 0. Since $Q(\cdot)$ is a monotonically decreasing function, we can analyze the performance of the term inside the parentheses instead. It is denoted as S in Section III. Then we can derive the first and second derivations of S with respect to N, the latter of which is given as follows

$$\begin{aligned} S''_N = & \frac{-\theta(k\gamma_p+1)^4}{4(r+(N-r)(\gamma_p+1)^2)^{\frac{3}{2}}\sqrt{g(k\gamma_p+1)^2+N-g}} \\ & - \frac{\frac{\theta(k\gamma_p+1)^2}{2\sqrt{r+(N-r)(k\gamma_p+1)^2}}+k\gamma_p}{(g(k\gamma_p+1)^2+N-g)^{3/2}} \\ & + \frac{3\theta\sqrt{r+(N-r)(k\gamma_p+1)^2}+(N-r-g)k\gamma_p}{4(g(k\gamma_p+1)^2+N-g)^{5/2}}. \end{aligned} \tag{30}$$

Suppose N is relatively large. It's hard to discern its concavity and convexity apparently due to uncertain r and g. To make the analysis mathematically tractable, we can divide the frame into three time subsections according to the moment of PU state change. Then by exploiting permutation and combination theory, we can deduce S''_N in the following nine possible representative situations according to the combinations of r and g to facilitate operation and comparison:

- $r \to N \,\&\, g \to N$. It represents that PU tends to change its state at the end of a frame period. It is the worst situation because the number of samples that can reflect the real state of PU is too small.
- $r \to N \,\&\, g \to N/2$. It indicates that PU usually arrives at the end of a frame but tends to leave in the middle of another frame.
- $r \to N \,\&\, g \to 0$. It means that PU usually appears during the last few samples of a frame but disappears early in another frame period.
- $r \to N/2 \,\&\, g \to N$. In this situation, PU is more likely to occur in the middle of a frame period but usually leaves at the end of another frame period.
- $r \to N/2 \,\&\, g \to N/2$. It describes the situation where PU usually changes its state halfway.
- $r \to N/2 \,\&\, g \to 0$. It represents that PU arrives in the middle of a frame but tends to departure at the beginning of another frame.
- $r \to 0 \,\&\, g \to N$. It corresponds to the situation that PU usually arrives at the beginning of a frame period but leaves at the end of another frame.
- $r \to 0 \,\&\, g \to N/2$. Similarly, it means that PU generally occurs at the beginning of a frame period but tends to disappear halfway.
- $r \to 0 \,\&\, g \to 0$. It represents that PU is more likely to change its state at the beginning of a frame period, which is the best situation since there are more samples making positive influence on sensing decision.

Note that the situations above are classified from a probabilistic point of view. By making such approximations of r and g, we can determine now that $S''_N < 0$. Then S is concave with respect to N. Considering the monotonically decreasing property of $Q(\cdot)$, and the definitions of concave and convex functions, we can infer that p_f is convex. Thus throughput is concave with respect to N (equivalent to T) in a very general way, which is validated in Section V. This means that for a certain p_{d_con}, there exists an optimal T which yields the maximum achievable throughput and the lowest p_f for SU.

Considering all possible moments of PU state change and adopted weighting schemes, we can formulate the following optimization problem:

$$\max_T \; R(T) \quad s.t. \begin{cases} P_d \geq P_{d\_con}, \\ T_{min} \leq T \leq T_{max}. \end{cases} \tag{31}$$

Here we constrain the practicable range of T to narrow down the search range. T_{min} and T_{max} should be determined appropriately according to specific requirement of system. In fact, too short T leads to too few samples, which impairs the sensing accuracy. But too long T may lead to serious interference and opportunity loss for being unable to detect the PU state change timely.

Though the throughput shows concavity with respect to T, the explicit expression of T_{opt} is hard to obtain in equation (31). Therefore, we propose an efficient search method by way of trichotomy based on the advance-retreat method [35]. The detail is shown in Algorithm 1. At first, the endpoints are set as the lower and upper bounds of T. Then we find two trisection points as candidate T that trisect the search interval, and calculate the corresponding achievable throughputs. If the throughput with the smaller trisection point is higher than that with the larger one, we update the search range by setting the upper bound of T as the larger trisection point. Or else we update the lower bound as the smaller trisection point. The iteration continues until the difference between lower and upper bounds is less than predefined resolution ϵ. Finally the optimal T is determined as the ultimate endpoint.

The number of iterations required depends on the resolution ϵ. Because the search range is shortened by one third after each iteration, it converges at an exponential rate. Then the minimum number of iterations n_{min} that making the difference between lower and upper bounds less than ϵ can be determined

Algorithm 1 Search for Optimum T_{opt}

Initialize: $a \leftarrow T_{min}$, $b \leftarrow T_{max}$
while $a + \epsilon < b$ **do**
  $mid \leftarrow a + (b-a)/3$, $midmid \leftarrow b - (b-a)/3$
  Calculate $R(mid)$, $R(midmid)$ using (25)
  if $R(mid) \geq R(midmid)$ **then**
    Update the search range: $b \leftarrow midmid$
  else
    Update the search range: $a \leftarrow mid$
  end if
end while
return Optimal T_{opt}: $T_{opt} \leftarrow a$

by (32), where $\lceil \cdot \rceil$ is the ceiling function

$$n_{min} = \left\lceil \ln\left(\frac{T_{max} - T_{min}}{\epsilon}\right) / \ln\left(\frac{3}{2}\right) \right\rceil. \tag{32}$$

Meanwhile, if the proposed adaptive weighting scheme is adopted, we can add the corresponding numerical search method into the throughput calculation in Step 4 to achieve the lowest p_f simultaneously, thus further improving the throughput.

F. Computational Complexity

Since the computational complexity of an addition, complex conjugation, or comparison operation is much lower than that of a multiplication operation, only multiplications are considered for simplicity. We assume that no fast exponential algorithm is exploited in our simulation. Detailed comparison of the computational complexities of different normalized weighting schemes is provided as follows.

Since energy detection is adopted, the computational complexity mainly includes two parts, i.e., setting threshold and calculating test statistics. Once an appropriate threshold is determined, every calculated test statistic is compared with it to make a decision.

From (18), the threshold can be obtained by solving the equation $P_d = P_{d\_con}$ with complexity $O(N^2)$. Note that the computational complexity of $Q(\cdot)$ can be omitted by using its lookup table.

The difference between different weighting schemes exists in the calculation of statistics. From (14), weights are multiplied with corresponding samples. Since the square of the magnitude requires N multiplications, the complexity of equal weighting scheme is $O(N)$.

For geometric sequence based weighting scheme [25], [26], $\sum_{i=1}^{N}(i+1)+1$ multiplications are required for any common ratio larger than 1. The additional multiplication is for normalizing the weighting coefficients. It's easy to derive that its complexity is $O(N^2)$.

With respect to the probability based weighting scheme [23], [24], it requires prior information of idle duration's distribution to get the probability of a PU appears at any sample. With presumed exponential distribution model, the test statistics can be obtained using $\sum_{i=1}^{N}(i+1)+1$ multiplications roughly. Thus, its complexity is also $O(N^2)$.

As for proposed weighting scheme with fixed power exponent f, $\sum_{i=1}^{N}(f+1)+1$ multiplications are necessary. Therefore, the complexity is reduced to $O(N)$. Since the adaptive weighting scheme adopts numerical search method to obtain the optimum f, it only needs several iterations to satisfy acquired iteration precision [35]. Every iteration leads to $O(N^2)$ complexity for calling and executing the threshold and P_f calculating module. Once the optimum f is selected, the complexity of the statistics calculation is the same with that of the scheme with fixed f.

In conclusion, our proposed weighting schemes will not increase the order of the computational complexity when compared to that of the geometric and the probability methods.

V. Numerical Results

In this section, simulation results are presented to evaluate the performance of different weighted sensing schemes by considering all possibilities of PU state change. Firstly, we analyze the performance of the proposed weighting scheme with both fixed and adaptive power exponents. To obtain the adapted optimum f, the $fminbnd$ routine of MATLAB optimization toolbox is used to solve the problem. Then, we compare our adaptive weighting scheme (denoted as power) with three normalized weighting schemes based on probability [23], [24] (denoted as probability), geometric sequence [25], [26] (denoted as geometric), and equal weighting (denoted as equal) over a wide range of SNRs. Since the common ratio significantly affects the performance of geometric sequence-based scheme, we consider the optimal ratio in simulations for fairness of comparison. Next, we evaluate the performance of these schemes with different T, in order to show the impact of frame duration on the frame structure of simultaneous sensing and transmission. Finally Algorithm 1 is conducted under different detection probability constraints with various PU traffic change rates to track the optimum duration.

The main parameters are presented as follows unless otherwise specified: $f_s = 6$ MHz, $P_{d\_con} = 0.99$, $k = 0.9$, $\gamma_s = 3$ dB. We are interested in low SNR regime with γ_p lower than 0 dB, and assume that $\gamma_{sp} = \gamma_p - 2$ dB, which can be estimated by spatial sensing [28] in specific networks.

A. Performance of the Proposed Weighting Schemes With Different Power Exponents

Firstly, we compare the false alarm probability of our proposed weighting scheme with both fixed and adaptive power exponents for various SNRs of received PU signal in Fig. 5. Empirically, we set $f_{max} = 40$ for the adaptive weighting scheme to narrow down the search rage. As for the activity of PU, we set the parameters of the duration of ON and OFF periods as $\lambda = \mu = 50$. For different SNRs, the detection threshold is determined by satisfying $P_d = P_{d\_con}$.

It can be seen that the false alarm probability is improved with γ_p. For the scheme with fixed f, the performance trends shift into reverse after γ_p increases to about -10 dB. When $\gamma_p < -10$ dB, smaller f can yield better performance. On the contrary, the system performance benefits from larger f when

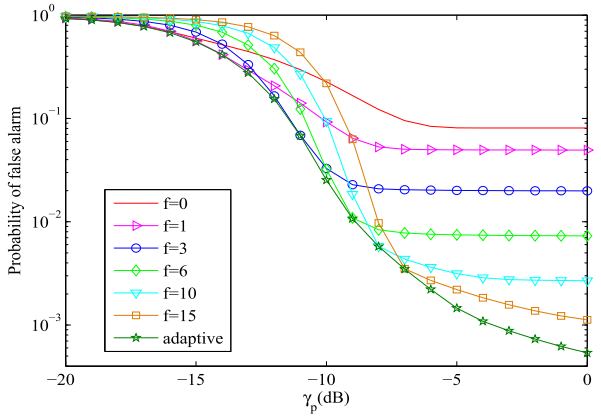

Fig. 5. Sensing performance of proposed scheme considering the PU state switch with different f. $\lambda = \mu = 50$, $T = 2$ ms.

$\gamma_p > -10$ dB. The reason is that, when SNR is too low, the difference between the samples of either an active or inactive PU is imperceptible. In this case, larger f may lead to instability due to larger variance of statistics, thus degrading the sensing performance. As SNR grows larger, using larger f can make the latest samples contribute more to the test statistics. We omit the cases of using larger f than 15, because their sensing performance deteriorates seriously in lower SNR environment. Nevertheless, the sensing performance with adaptive f achieves the best over the considered SNR range. In the following simulations, we adopt the adaptive weighting scheme for comparison and analysis.

B. Performance of Different Weighting Schemes With Different SNRs

In this subsection, we compare different weighting schemes in a wide range of SNR considering the PU state switch. With $\lambda = \mu = 80$, PU changes its state in each 12.5 ms, which implies that temporal spectrum holes are smaller compared with the above case, and in turn, the sensing duration shorter to make the decision timely, leading to the potential performance degradation.

The false alarm probability and throughput with different SNRs are shown in Fig. 6(a) and Fig. 6(b), respectively. The green line marked with plus represents proposed adaptive weighting scheme, which exhibits the lowest P_f and highest throughput, and requires lowest SNR to satisfy $P_f \leq 0.1$. The magenta line marked with circle indicates the geometric sequence-based weighting scheme. Its optimum common ratio is obtained by manually trying and comparing. The brown line marked with diamond and red line without marks reflect the probability-based weighting scheme and the equal weighting scheme, respectively. Overlay approach is adopted for comparison with the original works. We also plot the interweave sharing based throughput of the proposed weighting scheme, which is shown as the green line marked with pentagram. As the SNR γ_p increases, the throughputs of all methods are improved at first because their detection performance is much improved at first. With γ_p gets larger, P_f has become low enough and the improvements of throughputs are very slight. Meanwhile, since we focus on the achievable throughput of

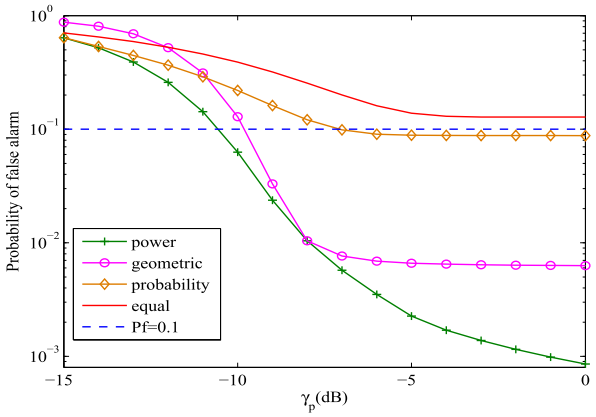

(a) Probability of false alarm

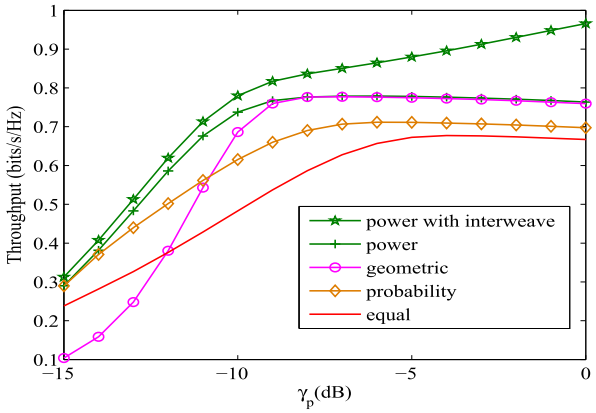

(b) Throughput

Fig. 6. Performance comparison of different weighting schemes when $T = 2$ ms, $\lambda = \mu = 80$.

SU, PU signal acts as a certain portion of noise during SU's transmission. Thus, the SNR of SU decreases accordingly, resulting in the slow decay of the throughputs of all methods except for the scheme of power with interweave. As for this scheme, when the sensing result indicates that PU is transmitting, SU can continue its transmission with an IFTP, which can be increased with γ_p [28]. Therefore, increasing the SNR γ_p improves its throughput.

C. Performance of Different Weighting Schemes With Various Frame Durations

We evaluate the performance of different weighting schemes with different frame durations. From previous simulation results, the performance of all schemes deteriorates when $\gamma_p \leq -10$ dB. Thus we set $\gamma_p = -10$ dB as a threshold.

Fig. 7 displays the sensing performance of these schemes. As can be seen, the proposed adaptive one exhibits the lowest P_f. With the increase of T, false alarm probabilities of both equal weighting and probability-based schemes improve when T grows from a small value and then decrease gradually when $T > 0.6$. Comparatively, both the geometric sequence based scheme and the proposed scheme gradually saturate when $T > 0.6$. In this case, increasing T can't always improve the performance since larger T induces longer delay periods.

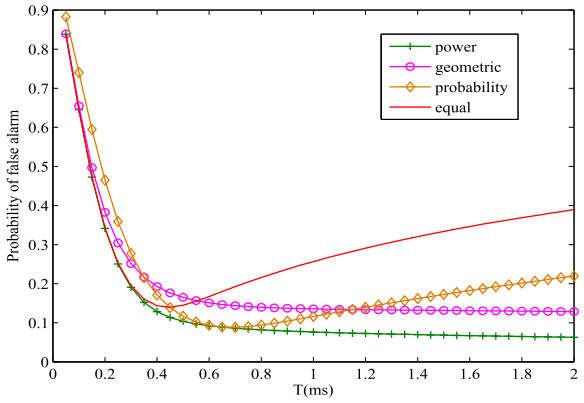

(a) False alarm probability when $\lambda = \mu = 80$

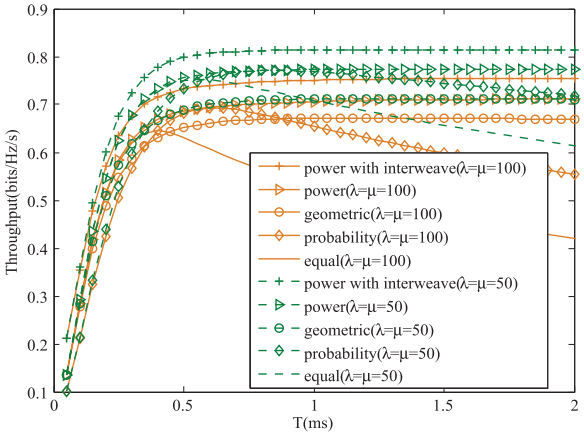

(b) Throughput

Fig. 7. Performance comparison of different weighting schemes when $\gamma_p = -10$ dB.

Thus, there exists an optimal T for each scheme with the adopted frame structure, with which the lowest P_f can be achieved.

The throughput of different weighting schemes with different T are illustrated in Fig. 7(b). We also plot the achievable throughput of the proposed scheme with interweave sharing. It can be seen that proposed schemes achieve higher throughput for different T, especially for our scheme with interweave sharing. The throughput of both the proposed adaptive weighting and geometric sequence-based weighting scheme eventually reach a plateau when T grows larger. While for the other two schemes, optimal T exist w.r.t maximizing the throughput. This result is consistent with that shown in Fig. 7(a).

With the increase of T, the consumed energy will certainly increase. The parameters for evaluating energy consumption are assumed as follows [34]: $\phi_c = 0.21$ W, $\phi_{se} = 0.1$ W, $\phi_{trs} = 0.31$ W, $\phi_{trsp} = 0.05$ W. Fig. 8 shows the energy efficiency of different schemes, where the proposed weighting scheme achieves the highest energy efficiency. Although the throughput of the proposed scheme with interweave sharing is higher than that with overlay sharing, the energy consumption is also increased, for it transmits even if PU is declared present. As a result, they shows indistinguishable performance. Besides, since the curves have optimal points with respect

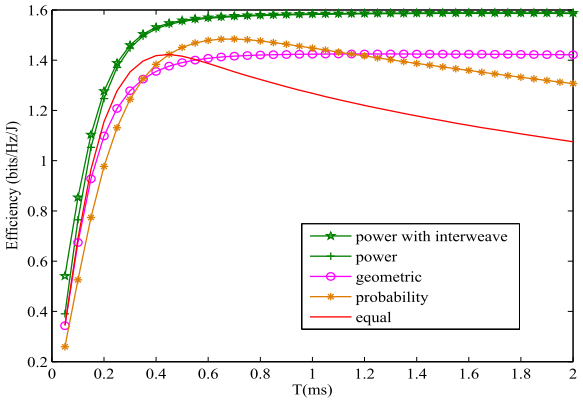

Fig. 8. Energy efficiencies of four sensing schemes varying with frame duration when $\lambda = \mu = 80$, $\gamma_p = -10$ dB.

to T, there's no need to increase T as long as the energy efficiency has reached the best.

Another important issue in CR system is the interference to PU. Since both the activity of PU and the sensing performance can influence the interference level, we also consider the situation of $\lambda = \mu = 20$ and $\lambda = \mu = 50$, respectively. From Fig. 9, we can see that the interference and outage increase with T. The reason is that longer T means larger delay to reflect possible PU state changes and higher possibility to encounter the reappearance of PU. In addition, the larger λ and μ are, the shorter PU state keeps, and therefore the more frequently PU state changes and more conflicts occur. That's why the interference and outage probabilities of the group with larger λ and μ are slightly higher than that with smaller ones. Besides, when $T \leq 0.8$ ms, the outage differences among the schemes are negligible. However, as analyzed in (23) and (24), the collision due to missed detection is low enough, the main factor from spectrum sensing is P_f. Thus with the increase of T, the proposed scheme displays marginally higher interference and outage than other schemes (Fig. 7(a)). Fortunately, we'll show in the following subsection that the optimum T of proposed scheme keeps within 0.8 ms, which will allay the concern.

D. Optimum Frame Duration

As illustrated above, there exists an optimum T for the structure of simultaneous sensing and transmission, with which the best throughput and energy efficiency can be achieved and the false alarm probability can be reduced concurrently. Therefore, we execute Algorithm 1 to search for the optimum T with specific P_{d_con} for the proposed weighted sensing scheme. Here we set the resolution as $\epsilon = 1$ μs. Then the results can be obtained after 19 iterations.

Fig. 10 illustrates the optimum T with different activities of PU varying with P_{d_con}. To indicate the situation where the durations of ON and OFF periods are unequal, we add two conditions with $\lambda = 60$, $\mu = 40$ and $\lambda = 40$, $\mu = 60$ as supplementary.

With the increase of λ or μ, the duration of PU's ON or OFF period becomes shorter, which means that the admissible optimum T of SU has to be shorter. While with the increase

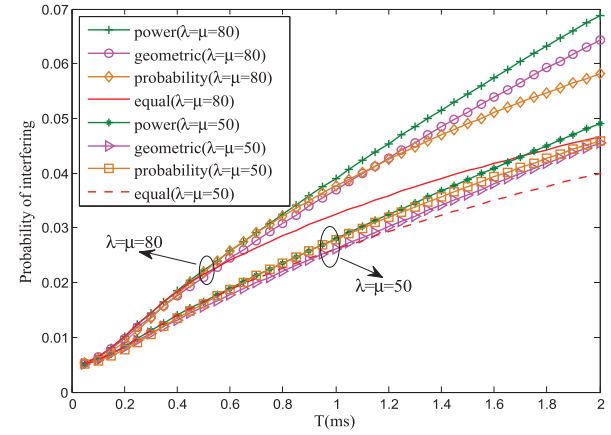

(a) Interference probability

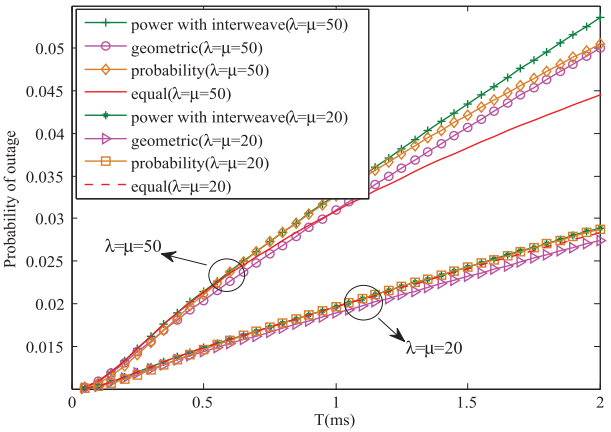

(b) Outage probability

Fig. 9. Performance comparison of different weighting schemes when $\gamma_p = -10$ dB.

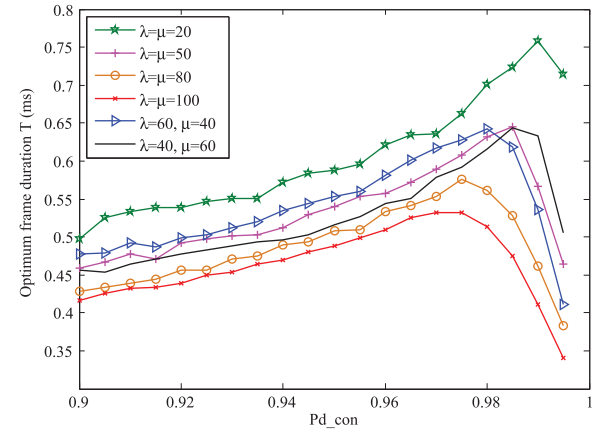

Fig. 10. Optimum frame duration varying with P_{d_con} when $\gamma_p = -10$ dB.

of P_{d_con}, the optimum T increases at first for it requires more samples to guarantee higher detection probability requirement. But it plunges when P_{d_con} increases to a certain value, and the optimal T in the situation with larger λ drops earlier than that with smaller one. That's because T can not increase infinitely in consideration of the duration of PU's ON (OFF) period, and therefore, when the required sensing duration can not be satisfied, the system sacrifices P_f by lowering down the threshold to achieve P_{d_con}. That's why P_f increases with P_{d_con}. Accordingly, the interference decreases with the reduction of missed detection probability. Furthermore, the increased P_f can lessen the opportunities of conflicts further. On the whole, with the optimal T, the collision probability can be kept within the tolerable range.

VI. Conclusion

A new weighted spectrum sensing scheme for the dynamic PU traffic environment with simultaneous data transmission was proposed in this paper. It could improve the performance over a wide range of SNR levels and adapt to the practical scenario. Compared with the existing works, the proposed scheme could characterize the PU state more accurately by allowing larger weights to the newer samples using a power function and achieve lowest false alarm probability through the adjusted power exponent. Moreover, considering all possibilities of PU state change, we analyzed the achievable average false alarm probability, interference, throughput and energy efficiency with various frame durations. Furthermore, the optimal frame duration yielding the optimal false alarm probability and throughput was computed. After that, a fast search algorithm was proposed to track the optimal frame duration. Simulation results were provided to validate the model and to demonstrate the improvement in low SNR. The results indicated that the proposed weighting scheme could achieve superior performance of sensing accuracy and energy efficiency in low SNR regime.

Acknowledgment

The authors would like to thank the anonymous reviewers and the associate editor for their constructive comments and Prof. J.Cai, Prof.H.Zhang, Prof.H.Chen, senior engineer H.L.Zhang and Prof. Y.M.Pan for their assistance in improving the presentation.

References

[1] J. Mitola and G. Q. Maguire, Jr., "Cognitive radio: Making software radios more personal," *IEEE Pers. Commun.*, vol. 6, no. 4, pp. 13–18, Apr. 1999.

[2] S. Haykin, "Cognitive radio: Brain-empowered wireless communications," *IEEE J. Sel. Areas Commun.*, vol. 23, no. 2, pp. 201–220, Feb. 2005.

[3] C. Yi and J. Cai, "Two-stage spectrum sharing with combinatorial auction and Stackelberg game in recall-based cognitive radio networks," *IEEE Trans. Commun.*, vol. 62, no. 11, pp. 3740–3752, Nov. 2014.

[4] T. Yucek and H. Arslan, "A survey of spectrum sensing algorithms for cognitive radio applications," *IEEE Commun. Surveys Tuts.*, vol. 11, no. 1, pp. 116–130, Mar. 2009.

[5] D. Cavalcanti and M. Ghosh, "Cognitive radio networks: Enabling new wireless broadband opportunities," in *Proc. Int. Conf. Cognit. Radio Oriented Wireless Netw. Commun. (CROWNCOM)*, Singapore, May 2008, pp. 1–6.

[6] Y.-C. Liang, Y. Zeng, E. C. Y. Peh, and A. T. Hoang, "Sensing-throughput tradeoff for cognitive radio networks," *IEEE Trans. Wireless Commun.*, vol. 7, no. 4, pp. 1326–1337, Apr. 2008.

[7] S. H. Song, K. Hamdi, and K. B. Letaief, "Spectrum sensing with active cognitive systems," *IEEE Trans. Wireless Commun.*, vol. 9, no. 6, pp. 1849–1854, Jun. 2010.

[8] M. H. P. Alves, R. A. A. de Souza, and A. J. Bragaz, "Simultaneous sensing-transmission in cognitive radio networks under spatiotemporally collaborative techniques," in *Proc. Eur. Conf. Antennas Propag. (EuCAP)*, Lisbon, Portugal, Apr. 2015, pp. 1–5.

[9] C. Wang and H. Chen, "A new signal structure for active sensing in cognitive radio systems," *IEEE Trans. Commun.*, vol. 62, no. 3, pp. 822–835, Mar. 2014.

[10] B. Zhao and S. Sasaki, "Active spectrum sensing for cognitive radio networks," *Trans. Emerg. Telecommun. Technol.*, vol. 26, no. 5, pp. 789–799, May 2015.
[11] Y. Liao, L. Song, Z. Han, and Y. Li, "Full duplex cognitive radio: A new design paradigm for enhancing spectrum usage," *IEEE Commun. Mag.*, vol. 53, no. 5, pp. 138–145, May 2015.
[12] J. I. Choi, M. Jain, K. Srinivasan, P. Levis, and S. Katti, "Achieving single channel, full duplex wireless communication," in *Proc. ACM Mobicom Conf.*, Chicago, IL, USA, Sep. 2010, pp. 1–12.
[13] E. Tsakalaki, O. N. Alrabadi, A. Tatomirescu, E. de Carvalho, and G. F. Pedersen, "Concurrent communication and sensing in cognitive radio devices: Challenges and an enabling solution," *IEEE Trans. Antennas Propag.*, vol. 62, no. 3, pp. 1125–1137, Mar. 2014.
[14] H. Chen, G. Li, and J. Cai, "Spectral–energy efficiency tradeoff in full-duplex two-way relay networks," *IEEE Syst. J.*, to be published. [Online]. Available: http://ieeexplore.ieee.org/stamp/stamp.jsp?arnumber=7219383
[15] T. Riihonen and R. Wichman, "Energy detection in full-duplex cognitive radios under residual self-interference," in *Proc. Int. Conf. Cognit. Radio Oriented Wireless Netw. Commun. (CROWNCOM)*, Oulu, Finland, Jun. 2014, pp. 57–60.
[16] J. Heo, H. Ju, S. Park, E. Kim, and D. Hong, "Simultaneous sensing and transmission in cognitive radio," *IEEE Trans. Wireless Commun.*, vol. 13, no. 4, pp. 1948–1959, Apr. 2014.
[17] S. Stotas and A. Nallanathan, "Overcoming the sensing-throughput tradeoff in cognitive radio networks," in *Proc. IEEE ICC*, Cape Town, South Africa, May 2010, pp. 1–5.
[18] S. Pandit and G. Singh, "Throughput maximization with reduced data loss rate in cognitive radio network," *Telecommun. Syst.*, vol. 57, no. 2, pp. 209–215, Oct. 2014.
[19] W. Cheng, X. Zhang, and H. Zhang, "Full-duplex spectrum-sensing and MAC-protocol for multichannel nontime-slotted cognitive radio networks," *IEEE J. Sel. Areas Commun.*, vol. 33, no. 5, pp. 820–831, May 2015.
[20] S. K. Sharma, S. Chatzinotas, and B. Ottersten, "A hybrid cognitive transceiver architecture: Sensing-throughput tradeoff," in *Proc. Int. Conf. Cognit. Radio Oriented Wireless Netw. Commun. (CROWNCOM)*, Oulu, Finland, Jun. 2014, pp. 143–149.
[21] V. V. Gowravajhala, "Simultaneous sense and access for cognitive radio networks: A throughput optimization perspective," in *Proc. Int. Wireless Commun. Mobile Comput. Conf. (IWCMC)*, Dubrovnik, Croatia, Aug. 2015, pp. 892–898.
[22] W. Afifi and M. Krunz, "Incorporating self-interference suppression for full-duplex operation in opportunistic spectrum access systems," *IEEE Trans. Wireless Commun.*, vol. 14, no. 4, pp. 2180–2191, Apr. 2015.
[23] J. Ma, X. Zhou, and G. Y. Li, "Probability-based periodic spectrum sensing during secondary communication," *IEEE Trans. Commun.*, vol. 58, no. 4, pp. 1291–1301, Mar. 2010.
[24] S. Chen, S. Gu, K. Li, and P. Dong, "Spectrum sensing performance analysis based on primary user probability access/leave model," in *Proc. Int. Conf. Autom., Mech. Control Comput. Eng. (AMCCE)*, Jinan, China, Apr. 2015, pp. 1964–1969.
[25] X. Yan *et al.*, "Improved energy detector for full duplex sensing," in *Proc. IEEE Veh. Technol. Conf. (VTC Fall)*, Vancouver, BC, Canada, Sep. 2014, pp. 1–5.
[26] W. Prawatmuang, D. K. C. So, and E. Alsusa, "Sequential cooperative spectrum sensing technique in time varying channel," *IEEE Trans. Wireless Commun.*, vol. 13, no. 6, pp. 3394–3405, Jun. 2014.
[27] A. Baghel and A. Trivedi, "On spectrum utilization in CRN using sequential sensing applying adaptive weighting in time varying channel," in *Proc. Int. Conf. Adv. Comput., Commun. Informat. (ICACCI)*, Kochi, Japan, Aug. 2015, pp. 161–165.
[28] B. L. Mark and A. O. Nasif, "Estimation of maximum interference-free power level for opportunistic spectrum access," *IEEE Trans. Wireless Commun.*, vol. 8, no. 5, pp. 2505–2513, May 2009.
[29] H. Urkowitz, "Energy detection of unknown deterministic signals," *Proc. IEEE*, vol. 55, no. 4, pp. 523–531, Apr. 1967.
[30] A. Mariani, A. Giorgetti, and M. Chiani, "Effects of noise power estimation on energy detection for cognitive radio applications," *IEEE Trans. Commun.*, vol. 59, no. 12, pp. 3410–3420, Dec. 2011.
[31] A. Ghasemi and E. S. Sousa, "Optimization of spectrum sensing for opportunistic spectrum access in cognitive radio networks," in *Proc. IEEE Consum. Commun. Netw. Conf. (CCNC)*, Las Vegas, NV, USA, Jan. 2007, pp. 1022–1026.
[32] L. Tang, Y.-F. Chen, E. L. Hines, and M.-S. Alouini, "Effect of primary user traffic on sensing-throughput tradeoff for cognitive radios," *IEEE Trans. Wireless Commun.*, vol. 10, no. 4, pp. 1063–1068, Apr. 2011.
[33] W.-Y. Lee and I. F. Akyildiz, "Optimal spectrum sensing framework for cognitive radio networks," *IEEE Trans. Wireless Commun.*, vol. 7, no. 10, pp. 3845–3857, Oct. 2008.
[34] Y. Pei, Y.-C. Liang, K. C. Teh, and K. H. Li, "Energy-efficient design of sequential channel sensing in cognitive radio networks: Optimal sensing strategy, power allocation, and sensing order," *IEEE J. Sel. Areas Commun.*, vol. 29, no. 8, pp. 1648–1659, Sep. 2011.
[35] S. Boyd and L. Vandenberghe, *Convex Optimization*. Cambridge, U.K.: Cambridge Univ. Press, 2004.

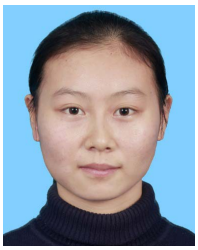

Min Deng was born in Hunan, China. She received the B.E. degree in communication engineering from Hunan University, Hunan, in 2010. She is currently pursuing the Ph.D. degree in information and communication engineering with the School of Electronic and Information Engineering, South China University of Technology, Guangzhou, China. Her research interests include cognitive radio technology, vehicular ad hoc networks, and wireless communication.

Bin-Jie Hu (M'08–SM'12) was born in Shanxi, China. He received the M.S. degree from the China Research Institute of Radiowave Propagation, Henan, China, in 1991, and the Ph.D. degree from the University of Electronic Science and Technology of China, Sichuan, China, in 1997, all in electronic engineering.

From 1997 to 1999, he was a Post-Doctoral Fellow with the South China University of Technology, Guangzhou, China. From 2001 to 2002, he was a Visiting Scholar with the Department of Electronic Engineering, City University of Hong Kong. He was a Visiting Professor with the Université de Nantes, France, in 2005. He is currently a Full Professor with the South China University of Technology. His current research interests include wireless communications, cognitive radios, vehicular ad hoc networks, and microwave circuits and antennas.

Xiaohuan Li was born in Chongqing, China. He received the B.Eng. and M.Sc. degrees from the Guilin University of Electronic Technology, Guilin, China, in 2006 and 2009, respectively, and the Ph.D. degree from the South China University of Technology, Guangzhou, China, in 2015.

He was a Visiting Scholar with the Université de Nantes, France, in 2014. He is currently an Associate Professor with the School of Information and Communication, Guilin University of Electronic Technology. His current research interests include wireless sensor networks, vehicular ad hoc networks, and cognitive radios.